Contact thermal resistance between silver nanowires with polyvinylpyrrolidone interlayers

Matthew L. Fitzgerald,[1] Yang Zhao,[1] Zhiliang Pan,[1] Lin Yang,[1] Shihong Lin,[2] Godfrey Sauti,[3] and Deyu Li[1,*]

[1]*Department of Mechanical Engineering, Vanderbilt University, Nashville, TN, 37235, USA*
[2]*Department of Civil and Environmental Engineering, Vanderbilt University, Nashville, TN 37235, USA*
[3]*NASA Langley Research Center, Hampton, VA 23681-2199, USA*

[*]Corresponding author: deyu.li@vanderbilt.edu

Abstract:

Various nanofillers have been adopted to enhance the thermal conductivity of polymer nanocomposites. While it is widely believed that the contact thermal resistance between adjacent nanofillers can play an important role in limiting thermal conductivity enhancement of composite materials, lack of direct experimental data poses a significant challenge to perceiving the effects of these contacts. This study reports on direct measurements of thermal transport through contacts between silver nanowires (AgNWs) with a polyvinylpyrrolidone (PVP) interlayer. The results indicate that a PVP layer as thin as 4 nm can increase the total thermal resistance of the contact by up to an order of magnitude when compared to bare AgNWs, even with a larger contact area. On the other hand, the thermal boundary resistance for PVP-silver interfaces could be significantly lower than that between polymer-carbon nanotubes (CNTs). Analyses based on these understandings further show why AgNWs could be more effective nanofillers than CNTs.

Keywords: nanocomposites, contact thermal resistance, Kapitza resistance, silver nanowires, polymer composites

Polymers are widely used materials due to their abundance, desirable mechanical properties, and relatively low cost; however, the normally low thermal conductivity of polymers (~0.1 W/m-K) limits their applications in electronic devices and heat exchangers where efficient heat transfer is essential. Not surprisingly, extensive efforts have been put forth in seeking thermally conductive polymer composites, and over a half-century of research has been devoted to improving composite thermal conductivity by introducing thermally conductive fillers into host polymeric matrices.[1,2] These polymer composites have been implemented in a variety of systems such as sensors,[3] flexible electronics,[4] and thermal interface materials,[5] where heat dissipation is critical to device performance. However, so far the overall thermal conductivity improvement of many polymer composites remains quite limited.

One notable example is CNT-polymer composites. Despite the exceptionally high thermal conductivity of CNTs (> 3,000 W/m-K for high quality, thin tubes),[6,7] many studies with CNTs embedded in a polymer matrix only show marginal thermal conductivity enhancement (< 1 W/m-K), significantly lower than that predicted based on particle mixing theory.[8,9] For CNTs and other fillers randomly dispersed in a polymer matrix, the primary hurdle for enhancing the thermal conductivity has been thought to be the contact thermal resistance that exists between adjacent fillers and between the filler and polymer. In fact, it has been experimentally demonstrated that the contact thermal resistance between individual multi-wall CNTs (MWCNTs) is much larger than the normally expected value as a result of the ~200 nm long phonon mean free path along the inter-layer direction of MWCNTs (or *c*-axis of graphite) and phonon reflection from the innermost tube layer.[10]

On the other hand, recent experimental results indicate that the contact thermal resistance between individual silver nanowires (AgNWs) could be ~20 times lower than that between similar

diameter MWCNTs.[11] In terms of thermal conductance per unit area, the value for contacts between AgNWs could be one order of magnitude higher than that between MWCNTs, which is partly due to lack of electron reflection back into the emitting wires.[10,11] This is consistent with the higher thermal conductivity values typically displayed by polymer composites utilizing metallic nanofillers.[12,13]

However, one outstanding issue is that in nanocomposites the contact morphology between nanofillers could be much more complex, and instead of direct contacts between nanofillers, there is often a thin polymer layer between neighboring nanofillers.[14] This thin polymer interlayer could enlarge the effective contact area between nanofillers but also poses additional thermal resistance. As such, it is important to explore how polymer interlayers alter the contact thermal resistance between nanofillers to better understand thermal transport in nanocomposites. This work presents measurements of contact thermal resistance between individual AgNWs with a thin PVP interlayer.

All thermal measurements were conducted using the well-established, micro-thermal bridge method in a cryostat (Janis CCS-400/204) under high vacuum ($<1\times10^{-6}$ mbar), which has been used to investigate thermal transport through various nanowires, including MWCNTs and AgNWs.[15-20] A Wheatstone bridge circuit was adopted to cancel the baseline cryostat temperature fluctuation, leading to a thermal conductance measurement resolution of ~ 85 pW/K at room temperature with the selected instrument settings.[21] The background thermal conductance between the suspended membranes was measured and subtracted from the total thermal conductance to further increase measurement accuracy (See supporting information). For the contact measurements, PVP was chosen as the polymer interlayer because of its affinity with silver.[22] To

explore the contact thermal resistance between AgNWs with a PVP interlayer, electrospun PVP nanofibers were first measured to determine their thermal conductivity.

To prepare PVP nanofibers, PVP powder (Sigma Aldrich, 437190-25G, molecular weight: 1,300 kg/mol) was dissolved in ethanol (Sigma Aldrich, 187380-1L) at a ratio of 1:10 (w/w), and the resulting solution was drawn into a 10 mL syringe through a 20-gauge needle. Electrospinning was conducted at a 20 kV operating voltage with a 50 μl/min flow rate, and the distance between the syringe tip and the grounded collector was 15 cm (See supporting information for more details).

Fig. 1a displays a scanning electron microscopy (SEM) image of an electrospun PVP nanofiber on the measurement device, while Fig. 1b shows the measured thermal conductivity of PVP nanofibers with different diameters and suspended lengths. The average thermal conductivity at 300 K was measured to be 0.23 ± 0.02 W/m-K, and no obvious trend exists for the various suspended lengths and diameters, indicating negligible contact thermal resistance between the suspended PVP fibers and the heat source/sink.[17,20]

The measured nanofiber thermal conductivity is slightly lower than that of PVP thin films prepared by spin-casting of PVP solution (molecular weight: 25 kg/mol) as reported by Xie et al.[23] This indicates that the thermal conductivity of the PVP nanofibers experiences little enhancement as a result of electrospinning, in contrast to the case of polyethylene.[17] However, it has been shown that for polymers with side groups of either a high molecular weight or large degrees of asymmetry, the chain alignment effect on the thermal conductivity of electrospun nanofibers tends to be adversely impacted.[20] As such, the heavy and complex side group of PVP (Fig. 1b inset) renders the effect of electrospinning on its thermal conductivity marginal, and the measured thermal conductivity of the PVP nanofibers is treated as the value for PVP in all calculations, no matter

what form the polymer takes. This is reasonable even for nanometers thick films considering that the phonon mean free path in PVP is only ~ 0.7 nm.[24]

To explore the contact thermal resistance between AgNWs with a PVP interlayer, a small amount of AgNWs (Sigma Aldrich, 739448-25ML) were placed in a solution of 1% by weight PVP in ethanol. After remaining in solution overnight (~16 hours), it was observed that the viscous polymer solution would adhere to the AgNW surfaces after removal and remain liquid for a long enough time to form a meniscus between two AgNWs placed in contact (See supporting information). By drop-casting the AgNW suspension onto a piece of polydimethylsiloxane (PDMS), individual nanowires could be identified and transferred to the thermal measurement device with a sharp probe mounted on an in-house built micromanipulator.

For the thermal measurement, a single PVP-coated AgNW with a length of > 80 μm was identified and broken into three segments, one to serve as a continuous reference sample (Fig. 2a) with the other two aligned to form a "contact sample" with a point contact between the suspended membranes (Fig. 2b). Here, due to the pentagonal cross-section of the AgNWs, the hydraulic diameter is adopted ($D_h = 4A/P$, where A is cross-sectional area and P is perimeter) to represent the characteristic dimension of the wire,[11] and the reported D_h is based on the silver core size without the PVP layer. Importantly, after thermal characterization, the contact samples were transferred to a piece of Si wafer, and focused ion beam (FIB) was used to cut the approximate center of the contact region, exposing the cross-section and allowing for estimation of the contact morphology (See supporting information). The SEM micrograph of the cross-section at the contact is shown in Fig. 2b.

Two sets of samples of 84 nm and 91 nm diameters, respectively, were measured, and the total thermal resistance of the contact and continuous wire samples is shown in Fig. 2c. From the cross-

sectional view of the contact region, the PVP interlayer thicknesses are estimated as 4 nm for the 84 nm diameter sample and 6 nm for the 91 nm diameter sample. This suggests that the PVP layers on the individual wire are 2 and 3 nm thick, respectively. The samples were prepared within one hour after the AgNW suspension was drop-cast on the PDMS, and due to the formation of the meniscus at the contact region, it is assumed that the PVP layers between the two AgNWs are fused together at the contact to form one layer of PVP.

Through careful probe operation, the suspended AgNW lengths between the two membranes for the continuous wire sample and the contact sample for each sample set were adjusted to be approximately the same. The measured total thermal resistance for these two samples can be expressed as

$$R_{t,s} = R_M + R_{w,s}, \quad (1)$$

$$R_{t,c} = R_M + R_{w,c} + R_c. \quad (2)$$

Here $R_{t,s}$ and $R_{t,c}$ denote the measured total thermal resistance of the continuous wire and the contact sample, respectively. R_M is the total thermal resistance between the nanowire and the two suspended membranes. $R_{w,s}$ and $R_{w,c}$ represent the intrinsic resistance of the nanowire in the continuous wire and the contact sample, respectively. Finally, R_c is the resistance of the contact between the two nanowires, which can be further written as $R_c = 2R_i + R_{PVP}$, where R_i is the interfacial thermal resistance between silver and PVP, while R_{PVP} denotes the thermal resistance of the PVP layer.

To extract R_c from the above equations, R_M is first considered. Recently, the thermal conductivity of individual, bare AgNWs of different diameters has been reported with careful confirmation that R_M is reduced to a negligible level.[11] As such, the thermal conductivity of the

bare AgNWs from that study can be treated as the intrinsic wire property. The measured thermal conductivity of PVP-coated AgNWs here is lower than the intrinsic value (see supplementary Fig. S3), and the difference can be attributed to the non-negligible R_M in the current measurement. Therefore, R_M can be solved based on Eq. (1) through calculating $R_{w,s}$ with the intrinsic wire thermal conductivity. For the 84 nm sample, a bare AgNW of the same diameter has been previously measured, and R_M is estimated from Eq. (1) as 9.82×10^5 K/W, or ~6% of $R_{t,s}$.

With non-negligible R_M, it is important to ensure that the thermalization distance, i.e., the distance required for the nanowire to reach thermal equilibrium with the membrane, is shorter than the actual length the samples are contacting the suspended membranes. Based on a fin model,[25] R_M can be written as

$$R_M = \frac{2}{\sqrt{hw_c\kappa_s A_s}\tanh\left(L_c\sqrt{\frac{hw_c}{\kappa_s A_s}}\right)}, \quad (3)$$

where h is the thermal conductance per unit area between the sample and the suspended membrane, w_c is the contact width, κ_s is the sample thermal conductivity, A_s is the sample cross-sectional area, and L_c is the contact length. Because $\tanh(x)$ asymptotically approaches unity as x increases and already reaches a value of 0.964 for x=2, it is reasonable to assume that a minimum thermalization distance, $L_{c,min}$, can be estimated by $L_{c,min} = 2\sqrt{\frac{\kappa_s A_s}{hw_c}}$.

The contact between the AgNW and suspended membranes occurs through one surface of the PVP-coated, pentagonal nanowire, with the 84 nm diameter wire having a 2 nm thick PVP layer. As such, the thermal conductance for the Ag-PVP-Pt composite interface can be estimated as $h = \left(\frac{2\,nm}{\kappa_{PVP}} + 2R_i''\right)^{-1}$. Note that the thermal boundary resistances for unit area (R_i'') at the PVP-silver and PVP-platinum interfaces are assumbed to be approximately the same, which is reasonable

considering that electron-phonon coupling on the metal side dominates the interfacial thermal resistance.[26,27] While R_i'' for PVP and metal is not available, a typical value of 1×10^{-8} m^2-K/W is assumed, which is based on the value recently reported for metal-polymethyl methacrylate interfaces.[28] For the PVP layer, the thermal conductivity measured in this study is used, which yields h=3.48 × 10^7 W/m^2-K at room temperature. Now, the contact width of the 84 nm diameter wire is 58 nm and using the intrinsic thermal conductivity of AgNWs from Zhao et al.'s measurement, $L_{c,min}$ is estimated as 2.03 μm. For the 84 nm sample, the minimum contact length is 3.37 μm, which is beyond $L_{c,min}$. Actually, R_M calculated from Eq. (3) is 9.75 × 10^5 K/W, which compares very well with the 9.82 × 10^5 K/W as previously derived using Eq. (1). Similar conclusions can be drawn for the 91 nm diameter wire (see the supporting information).

The above analysis indicates that R_M is approximately the same for both the continuous wire and contact samples, allowing for extraction of R_c through subtracting Eq. (1) from Eq. (2). For the 84 nm sample, the lengths of the suspended AgNWs for the single wire and contact sample are both ~28 μm, which leads to $R_c = R_{t,c} - R_{t,s}$. However, for the 91 nm sample the two AgNW segments in the contact sample are slightly longer than that of the continuous wire, 29 μm *versus* 27 μm. In this case, $R_{t,s}$ is scaled to account for the length difference and $R_c = R_{t,c} - R_{t,s} \times 29/27$. This inevitably introduces some error because the scaling also applies to R_M; however, since R_M for the 91 nm sample is ~13% of the total resistance, the above approach only introduces a small error.

At 300 K, R_c is found to be 6.55 × 10^6 K/W and 7.71 × 10^6 K/W for the 84 nm and 91 nm samples, respectively. Interestingly, despite the presence of the PVP interlayer, these R_c values are lower than the ~1.3 × 10^7 K/W reported for the point contact between two 68 nm diameter MWCNTs,[10] which suggests silver nanowires could be more effective for enhancing composites

thermal conductivity. To further understand thermal transport at the contact, the contact thermal resistance for unit area is calculated. At the contact, two flat, PVP-coated faces of the pentagonal AgNWs were observed to contact each other as shown in the inset of Fig. 2b, which leads to a parallelogram whose area (A_c) can be calculated with $A_c = \frac{{w_s}^2}{\sin\theta}$, where w_s is the width of the contact surface and θ is the contact angle. The contact angles were measured to be 55° and 54° for the 84 nm and 91 nm sample, with corresponding contact areas derived as 4,107 nm^2 and 4,984 nm^2, respectively. Thus, the area normalized contact thermal resistance (R_c'') values at 300 K are 2.69 × 10^{-8} m^2-K/W for the 84 nm sample and 3.84 × 10^{-8} m^2-K/W for the 91 nm sample. Fig. 2d also indicates that R_c'' decreases with temperature, which is largely determined by the lower PVP resistance as temperature escalates, as a result of the higher thermal conductivity of PVP at high temperatures. In addition, numerous studies have also shown the same trend for thermal boundary resistance,[10,26] which could exist between silver and PVP.

As mentioned previously, R_c contains contributions from the PVP interlayer, R_{PVP}, and the interfacial thermal resistance between PVP and silver, R_i. For unit contact area, the resistance of the PVP layer can be solved by $R''_{PVP} = t/\kappa_{PVP}$, where t is the thickness, and $R_i'' = (R_c'' - R''_{PVP})/2$, where a factor of 2 is introduced as there are two PVP-silver interfaces. The derived R_i'' is shown in Fig. 3a, and at 300 K, R''_i assumes an average value of 5.50 × 10^{-9} m^2-K/W. It is important to note that because the PVP interlayer thicknesses are approaching the SEM resolution, there is considerable uncertainty associated with the determination of R_i'' as indicated by the red shaded region in Fig. 3a. Nevertheless, the data is still able to shed light on aspects important to the design of polymer composites.

Firstly, R_c'' for the AgNW-PVP-AgNW contacts is much higher than the 8.26×10^{-11} m^2-K/W recently reported for Ag-Ag interfaces.[11] Moreover, despite the ~40 times larger contact area, R_c for the PVP coated AgNWs is still ~10 times higher than that reported for the contact between two 65 nm bare AgNWs (7.70×10^5 K/W). This indicates that it is critical for AgNWs to reach direct contacts to most effectively enhance composite thermal conductivity.

Moreover, even when considering the upper bound of the uncertainty, the derived interfacial thermal resistance between PVP and silver, R_i'', is lower than the typical values (1-8 $\times 10^{-8}$ m^2-K/W) for CNT-polymer systems as reported by a number of studies.[14,29-31] This difference in the thermal boundary resistance could contribute to an improved thermal conductivity enhancement with AgNWs. To demonstrate this, a generalized Maxwell-Garnett effective medium approximation (EMA)[30] was adopted to predict the thermal conductivity enhancement of bulk PVP-AgNW composites against previously reported CNT-polymer composites for which the model was used to fit experimental data and determine the interfacial thermal resistance.[9,31,32] According to the EMA, the thermal conductivity of a polymer composite with randomly dispersed, high aspect ratio rods can be descried as:[30]

$$\frac{\kappa_c}{\kappa_m} = \frac{3+\varphi(\beta_x+\beta_z)}{3-\varphi\beta_x}, \tag{4}$$

with

$$\beta_x = \frac{2(\kappa_{11}-\kappa_m)}{\kappa_{11}+\kappa_m}, \beta_z = \frac{\kappa_{33}}{\kappa_m} - 1. \tag{5}$$

Here κ_c and κ_m are the composite and polymer matrix thermal conductivity, respectively, and φ is the volume fraction of nanofillers. κ_{11} and κ_{33} are the equivalent nanofiller thermal conductivities

along the transverse and longitudinal axes, respectively, when including the effects of thermal boundary resistance according to:

$$\kappa_{11} = \frac{\kappa_f}{1+\frac{2R_i''\kappa_f}{d}}, \kappa_{33} = \frac{\kappa_f}{1+\frac{2R_i''\kappa_f}{L}}. \quad (6)$$

Here κ_f is the filler thermal conductivity and d and L are the nanofiller diameter and length.

Fig. 3b shows the predicted thermal conductivity enhancement (κ_c/κ_m) for a PVP-AgNW composite compared against the corresponding values for SWCNT and MWCNT composites as reproduced from the literature. It is important to note that Maxwell-Garnett type EMA models consider "thermally isolated" filler networks, and while CNTs have been shown to electrically percolate at low volume fractions, no corresponding thermal percolation has been observed,[9,31] which is consistent with the relatively large interfacial thermal resistance. Thus, the EMA model is considered valid at low volume fractions, and the linear profiles of thermal conductivity enhancement are consistent with enhancements observed for CNT-polymer composites.[9,31,32]

Interestingly, despite the lower thermal conductivity for silver, the AgNW-PVP composites drastically outperform previously measured CNT composites, and as indicated by the red shaded region in Fig. 3b, the uncertainty associated with R_i'' only has a minor effect on their predicted thermal conductivity enhancement. Examination of the model parameters suggests that the larger d and L of AgNWs (84 nm and 80 μm, respectively) and the lower R_i'' correspond to higher equivalent filler thermal conductivities (κ_{11} and κ_{33}), which renders AgNWs more effective nanofillers for thermal conductivity enhancement when randomly dispersed in a polymer matrix.

In summary, the contact thermal resistance between individual AgNWs with a PVP interlayer was measured in order to understand thermal transport through polymer composites. The results

indicate that the PVP layer leads to a significantly higher contact thermal resistance as compared to that between bare AgNWs, even though the contact area becomes much larger with PVP. A rather low interfacial thermal resistance between PVP and silver is derived which, combined with the larger wire size, renders AgNWs much more effective nanofillers than CNTs for enhancement of the thermal conductivity of polymer composites.

Associated Content

Supporting Information

The Supporting Information is available free of charge on the ACS Publications website (https://pubs.acs.org).

Sample preparation, measurement method, contact thermal resistance characterization, cross-sectional and contact area characterizations, and experimental uncertainty; Effective medium approximation (EMA) model parameters.

Acknowledgements

The authors thank the financial support from the U.S. National Science foundation (Award#1903645 and #1532107). M.L.F. acknowledges the graduate fellowship support from the National Aeronautics and Space Administration (NSTRF18_80NSSC18K1165). The work was performed in part at Cornell Nanoscale Facility, an NNCI member supported by NSF Grant NNCI-2025233.

Notes

The authors declare no competing financial interest.

References:

(1) Bigg, D.M. Thermally conductive polymer compositions. Polymer composites. **1986**, 7, 125-140.
(2) Chen, H.; Ginzburg, V.V.; Yang, J.; Yang, Y.; Liu, W.; Huang, Y.; Du, L.; Chen, B. Thermal Conductivity of Polymer-Based Composites: Fundamentals and Applications. *Prog. Polym. Sci*. **2016**, 59, 41-85.
(3) Wang, J.; Musameh, M. Carbon Nanotube/Teflon Composite Electrochemical Sensors and Biosensors. *Anal. Chem*. **2003**, 75, 2075-2079.
(4) Eda, G.; Chhowalla, M. Graphene-based Composite Thin Films for Electronics. *Nano Lett*. **2009**, 9, 814-818.
(5) Ngo, Q.; Cruden, B.A.; Cassell, A.M.; Sims, G.; Meyyappan, M.; Li J.; Yang, C.Y. Thermal Interface Properties of Cu-filled Vertically Aligned Carbon Nanofiber Arrays. *Nano Lett*. **2004**, 4, 2403-2407.

(6) Berber, S.; Kwon, Y.K.; Tománek, D. Unusually High Thermal Conductivity of Carbon Nanotubes. *Phys. Rev. Lett*. **2000**, 84, 4613.
(7) Kim, P.; Shi, L.; Majumdar, A.; McEuen, P.L. Thermal Transport Measurements of Individual Multiwalled Nanotubes. *Phys. Rev. Lett*. **2001**, 87, 215502.
(8) Biercuk, M.J.; Llaguno, M.C.; Radosavljevic, M.; Hyun, J.K.; Johnson, A.T.; Fischer, J.E. Carbon Nanotube Composites for Thermal Management. *App. Phys. Lett*. **2002**, 80, 2767-2769.
(9) Bryning, M.B.; Milkie, D.E.; Islam, M.F.; Kikkawa, J.M.; Yodh, A.G. Thermal Conductivity and Interfacial Resistance in Single-wall Carbon Nanotube Epoxy Composites. *App. Phys. Lett*. **2005**, 87, 161909.
(10) Yang, J.; Shen, M.; Yang, Y.; Evans, W.J.; Wei, Z.; Chen, W.; Zinn, A.A.; Chen, Y.; Prasher, R.; Xu, T.T.; Keblinski, P. Phonon Transport through Point Contacts Between Graphitic Nanomaterials. *Phys. Rev. Lett*. **2014**, 112, 205901.
(11) Zhao, Y.; Fitzgerald, M.L.; Tao, Y.; Pan, Z.; Sauti, G.; Xu, D.; Xu, Y.Q.; Li, D. Electrical and Thermal Transport through Silver Nanowires and their Contacts: Effects of Elastic Stiffening. *Nano Lett*. **2020**, 20, 7389-7396.
(12) Huang, X.; Jiang, P.; Xie, L. Ferroelectric Polymer/Silver Nanocomposites with High Dielectric Constant and High Thermal Conductivity. *App. Phys. Lett*. **2009**, 95, 242901.
(13) Balachander, N.; Seshadri, I.; Mehta, R.J.; Schadler, L.S.; Borca-Tasciuc, T.; Keblinski, P.; Ramanath, G. Nanowire-filled Polymer Composites with Ultrahigh Thermal Conductivity. *App. Phys. Lett*. **2013**, 102, 093117.
(14) Shenogin, S.; Xue, L.; Ozisik, R.; Keblinski, P.; Cahill, D.G. Role of Thermal Boundary Resistance on the Heat Flow in Carbon-nanotube Composites. *J. App. Phys*. **2004**, 95, 8136-8344.
(15) Li, D.; Wu, Y.; Kim, P.; Shi, L.; Yang, P.; Majumdar, A. Thermal Conductivity of Individual Silicon Nanowires. *App. Phys. Lett*. **2003**, 83, 2934-2936.
(16) Moore, A.L.; Shi, L. On Errors in Thermal Conductivity Measurements of Suspended and Supported Nanowires Using Micro-Thermometer Devices from Low to High Temperatures. *Meas. Sci. and Tech*. **2010**, 22, 015103.
(17) Ma, J.; Zhang, Q.; Mayo, A.; Ni, Z.; Yi, H.; Chen, Y.; Mu, R.; Bellan, L.M.; Li, D. Thermal Conductivity of Electrospun Polyethylene Nanofibers. *Nanoscale*. **2015**, 7, 16899-16908.
(18) Shi, L.; Li, D.; Yu, C.; Jang, W.; Kim, D.; Yao, Z.; Kim, P.; Majumdar, A. Measuring Thermal and Thermoelectric Properties of One-Dimensional Nanostructures Using a Microfabricated Device. *J. Heat Transfer*. **2003**, 125, 881-888.
(19) Yang, L.; Zhang, Q.; Cui, Z.; Gerboth, M.; Zhao, Y.; Xu, T.T.; Walker, DG.; Li, D. Ballistic Phonon Penetration Depth in Amorphous Silicon Dioxide. *Nano Lett*. **2017**, 17, 7218-7225.
(20) Zhang, Y.; Zhang, X.; Yang, L.; Zhang, Q.; Fitzgerald, M.L.; Ueda, A.; Chen, Y.; Mu, R.; Li D.; Bellan, L.M. Thermal Transport in Electrospun Vinyl Polymer Nanofibers: Effects of Molecular Weight and Side Groups. *Soft Matter*. **2018**, 14, 9534-9541.
(21) Wingert, M.C.; Chen, Z.C.; Kwon, S.; Xiang, J.; Chen, R. Ultra-sensitive Thermal Conductance Measurement of One-dimensional Nanostructures Enhanced by Differential Bridge. *Rev. Sci. Instrum*. **2012**, 83, 024901.
(22) Al-Saidi, W.A.; Feng, H.; Fichthorn, K.A. Adsorption of Polyvinylpyrrolidone on Ag Surfaces: Insight into a Structure-Directing Agent. *Nano Lett*. **2012**, 12, 997-1001.
(23) Xie, X.; Li, D.; Tsai, T.H.; Liu, J.; Braun, P.V.; Cahill D.G. Thermal Conductivity, Heat Capacity, and Elastic Constants of Water-Soluble Polymers and Polymer Blends. *Macromolecules*. **2016**, 49, 972-978.

(24) Choy CL. Thermal conductivity of polymers. *Polymer*. **1977**, 18, 984-1004.
(25) Bifano, M.F.; Park, J.; Kaul, P.B.; Roy, A.K.; Prakash, V. Effects of Heat Treatment and Contact Resistance on the Thermal Conductivity of Individual Multiwalled Carbon Nanotubes Using a Wollaston Wire Thermal Probe. *J. App. Phys*. **2012**, 111, 054321.
(26) Majumdar, A.; Reddy, P. Role of Electron–Phonon Coupling in Thermal Conductance of Metal–Nonmetal Interfaces. *App. Phys. Lett*. **2004**, 84, 4768-4770.
(27) Stevens, R.J.; Smith, A.N.; Norris, P.M. Measurement of Thermal Boundary Conductance of a Series of Metal-Dielectric Interfaces by the Transient Thermoreflectance Technique. *J. Heat Transfer*. **2005**, 127, 315-322.
(28) Sandell, S.; Maire, J.; Chávez-Ángel, E.; Torres, C.M.; Kristiansen, H.; Zhang, Z.; He, J. Enhancement of Thermal Boundary Conductance of Metal–Polymer System. *Nanomaterials*. **2020**, 10, 670.
(29) Huxtable, S.T.; Cahill, D.G.; Shenogin, S.; Xue, L.; Ozisik, R.; Barone, P.; Usrey, M.; Strano, M.S.; Siddons, G.; Shim, M.; Keblinski, P. Interfacial Heat Flow in Carbon Nanotube Suspensions. *Nat. Mater*. **2003**, 2, 731-734.
(30) Nan, C.W.; Liu, G.; Lin, Y.; Li, M. Interface Effect on Thermal Conductivity of Carbon Nanotube Composites. *App. Phys. Lett*. **2004**, 85, 3549-3551.
(31) Haggenmueller, R.; Guthy, C.; Lukes, J.R.; Fischer, J.E.; Winey, K.I. Single Wall Carbon Nanotube/Polyethylene Nanocomposites: Thermal and Electrical Conductivity. *Macromolecules*. **2007**, 40, 2417-2421.
(32) Kapadia, R.S.; Louie, B.M.; Bandaru, P.R. The Influence of Carbon Nanotube Aspect Ratio on Thermal Conductivity Enhancement in Nanotube–Polymer Composites. *J. Heat Transfer*. **2014**, 136.

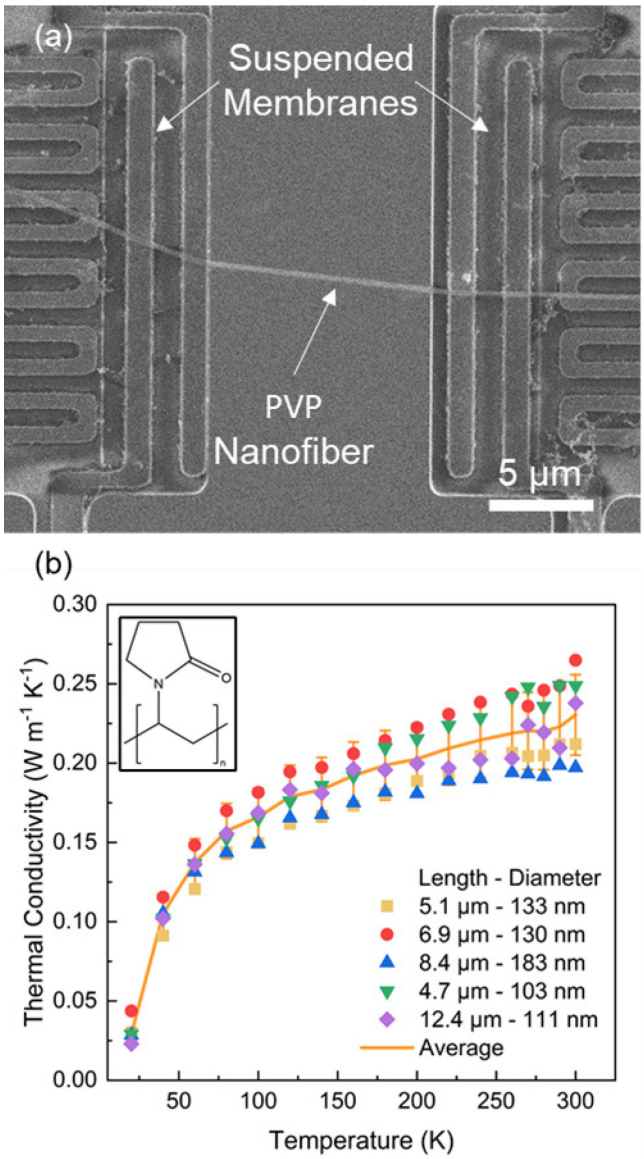

Figure 1: (a) An SEM micrograph of a 12.4 μm long electrospun PVP nanofiber placed on the thermal measurement microdevice. (b) The measured thermal conductivities of neat PVP fibers of various suspended lengths and diameters. The solid line represents the average thermal conductivity and associated measurement uncertainties are also indicated. The inset shows the chemical structure of PVP which has a chemical formula of $(C_6H_9NO)_n$.

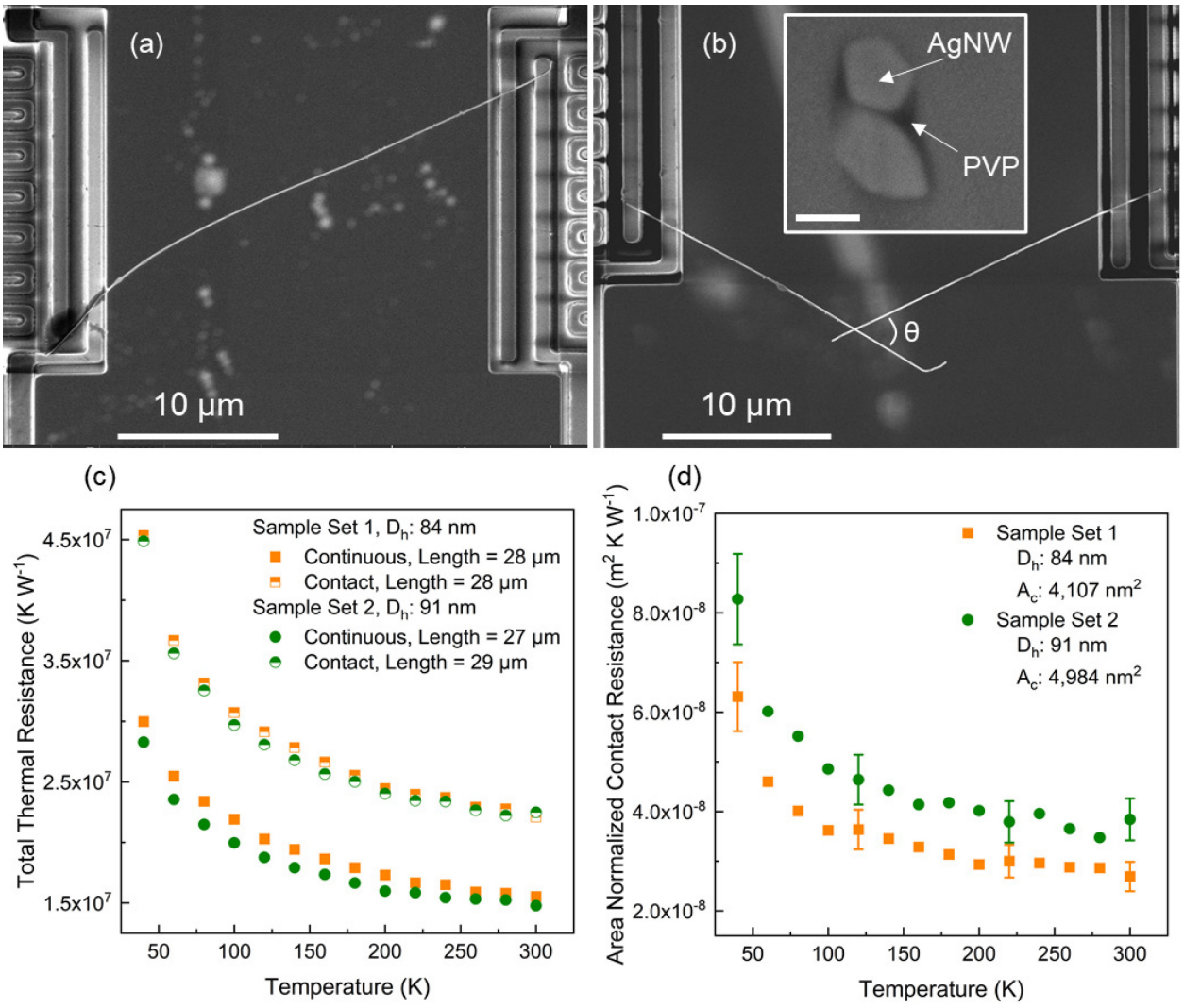

Figure 2: Contact thermal resistance between AgNWs with PVP interlayers. SEM micrographs of (a) an 84 nm diameter, PVP-coated AgNW and (b) the corresponding contact sample formed from two segments of the 84 nm PVP-coated AgNW. The inset shows an SEM micrograph of the contact cross-section after FIB milling. Inset scale bar is 80 nm. (c) Measured total thermal resistance of the contact and continuous samples. (d) Area normalized contact resistance for the 84 and 91 nm contact samples.

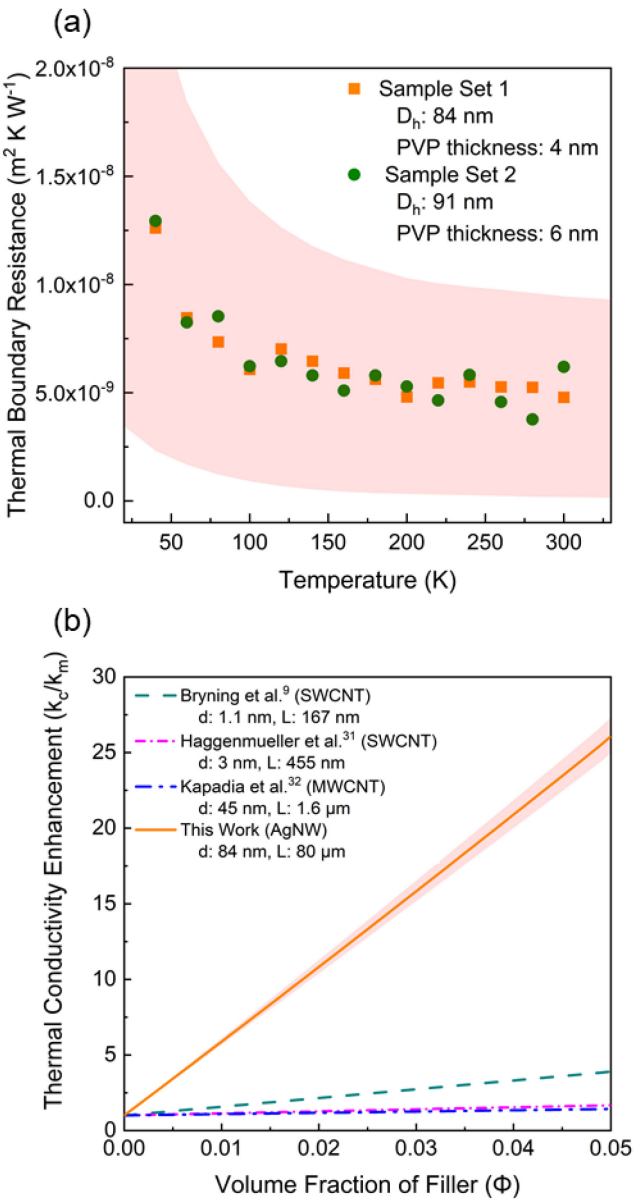

Figure 3: (a) Area normalized interfacial thermal resistance between PVP and silver. Note that the shaded region indicates the measurement uncertainty, and for clarity, nearest neighbor averaging is used to smooth the upper and lower bounds. (b) Predicted thermal conductivity enhancement (κ_c/κ_m) of AgNWs compared against effective media approximation (EMA) fits of experimental data reproduced from literature. Here the shaded region represents the upper and lower bounds of the EMA predictions corresponds to the boundary resistance range in (a).